LHCP 2024, June 5th 2024

# Higgs differential measurements and EFT interpretation in ATLAS

G. Callea on behalf of the ATLAS collaboration

"YOU ARE WELCOME HERE!"

# Introduction

Since its discovery, extensive studies on the Higgs properties have been carried out and used as a probe for the BSM scenario

The Nature paper (Nature 607, 52 (2022)) gives a fantastic overview of the ATLAS measurements, most of which were performed with the full Run2 dataset

| Decay mode | Targeted production processes | $\mathcal{L}$ [fb$^{-1}$] | Ref. | Fits deployed in |
|---|---|---|---|---|
| $H \to \gamma\gamma$ | ggF, VBF, $WH$, $ZH$, $t\bar{t}H$, $tH$ | 139 | [31] | All |
| $H \to ZZ$ | ggF, VBF, $WH + ZH$, $t\bar{t}H + tH$ | 139 | [28] | All |
| | $t\bar{t}H + tH$ (multilepton) | 36.1 | [39] | All but fit of kinematics |
| $H \to WW$ | ggF, VBF | 139 | [29] | All |
| | $WH$, $ZH$ | 36.1 | [30] | All but fit of kinematics |
| | $t\bar{t}H + tH$ (multilepton) | 36.1 | [39] | All but fit of kinematics |
| $H \to Z\gamma$ | inclusive | 139 | [32] | All but fit of kinematics |
| $H \to b\bar{b}$ | $WH$, $ZH$ | 139 | [33, 34] | All |
| | VBF | 126 | [35] | All |
| | $t\bar{t}H + tH$ | 139 | [36] | All |
| | inclusive | 139 | [37] | Only for fit of kinematics |
| $H \to \tau\tau$ | ggF, VBF, $WH + ZH$, $t\bar{t}H + tH$ | 139 | [38] | All |
| | $t\bar{t}H + tH$ (multilepton) | 36.1 | [39] | All but fit of kinematics |
| $H \to \mu\mu$ | ggF + $t\bar{t}H + tH$, VBF + $WH + ZH$ | 139 | [40] | All but fit of kinematics |
| $H \to c\bar{c}$ | $WH + ZH$ | 139 | [41] | Only for free-floating $\kappa_c$ |
| $H \to$ invisible | VBF | 139 | [42] | $\kappa$ models with $B_{u.}$ & $B_{inv.}$ |
| | $ZH$ | 139 | [43] | $\kappa$ models with $B_{u.}$ & $B_{inv.}$ |

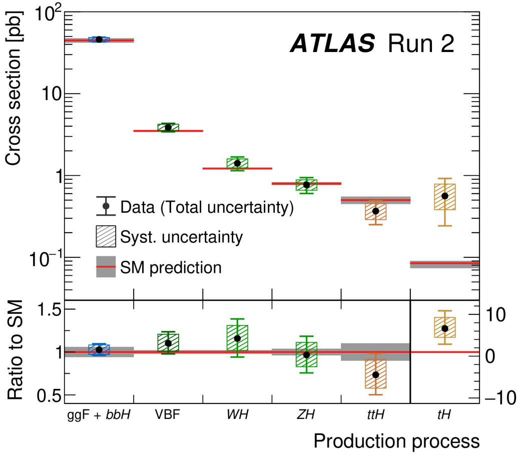


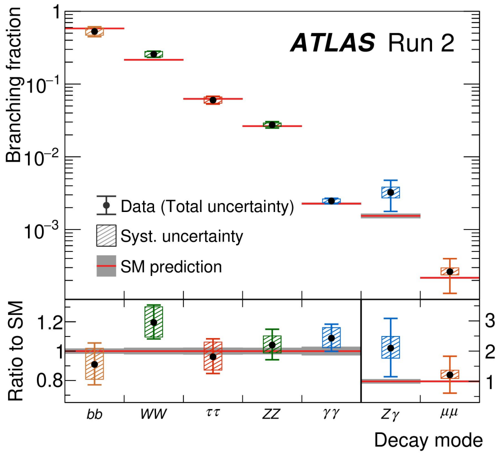

# Cross-section measurements & k-framework

- *Fiducial and differential measurements*: Done in specific phase-space regions. Shape information can be exploited for a range of further interpretations
- *Simplified template cross-section (STXS)*: Performed in prescribed bins per production mode, kinematic regions defined by the Higgs and associated W, Z or jets
- *kappa-framework*: set of coupling strength modifiers to express modification with respect to SM predictions and probe possible BSM

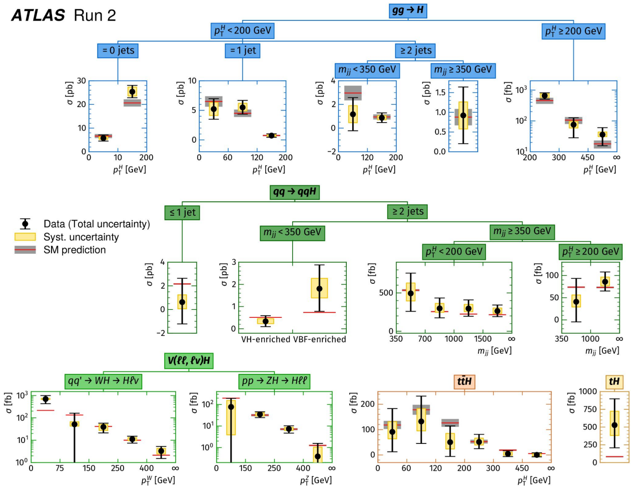


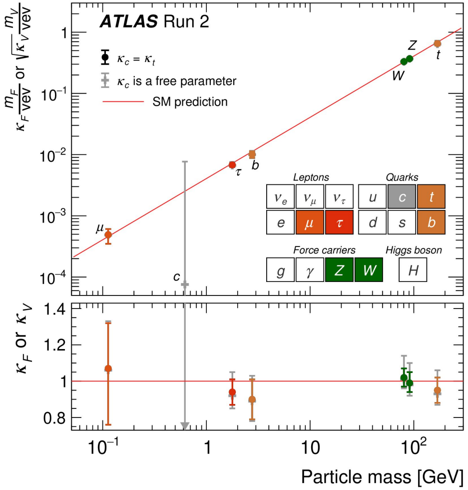

# H→ZZ (4l) and H→ γγ - Fiducial and total cross section

JHEP 05 (2023) 028

Excellent signal resolution but low event counts, individually -> Combination using Run2 data

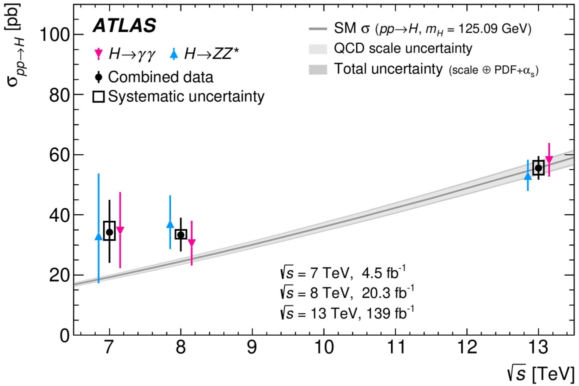


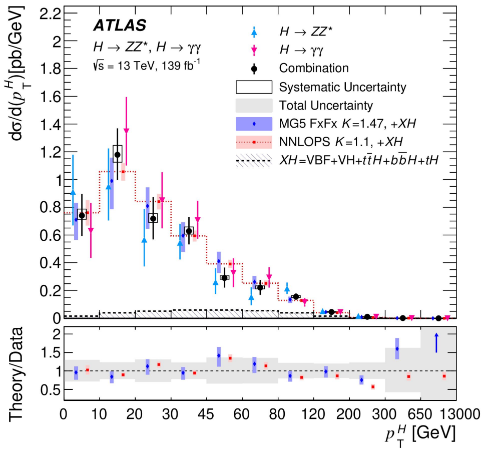


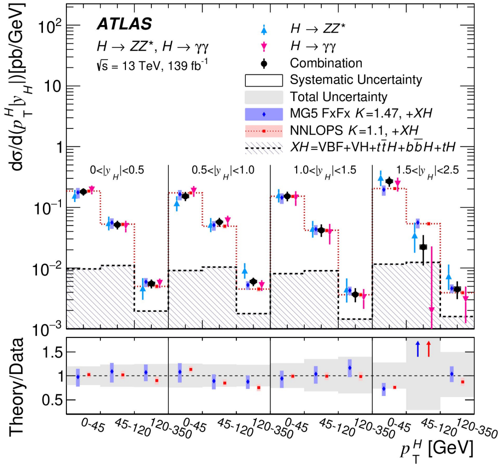


- Total Higgs production cross section measured with unprecedented precision of 7%
- Differential cross-section as a function of $p_T$ measured with 20-30% (60%) precision up to 300 GeV (350-650 GeV)

# H→ZZ (4l) and H→ γγ

JHEP 05 (2023) 028

The $p_T^H$ distribution is sensitive to modification of Yukawa couplings with the b- and c-quarks:

- Resulting in changes to overall cross section and shape of the $p_T^H$ distribution
- Affecting the H→ZZ and H→γγ branching ratios with the changes in the Higgs decay width

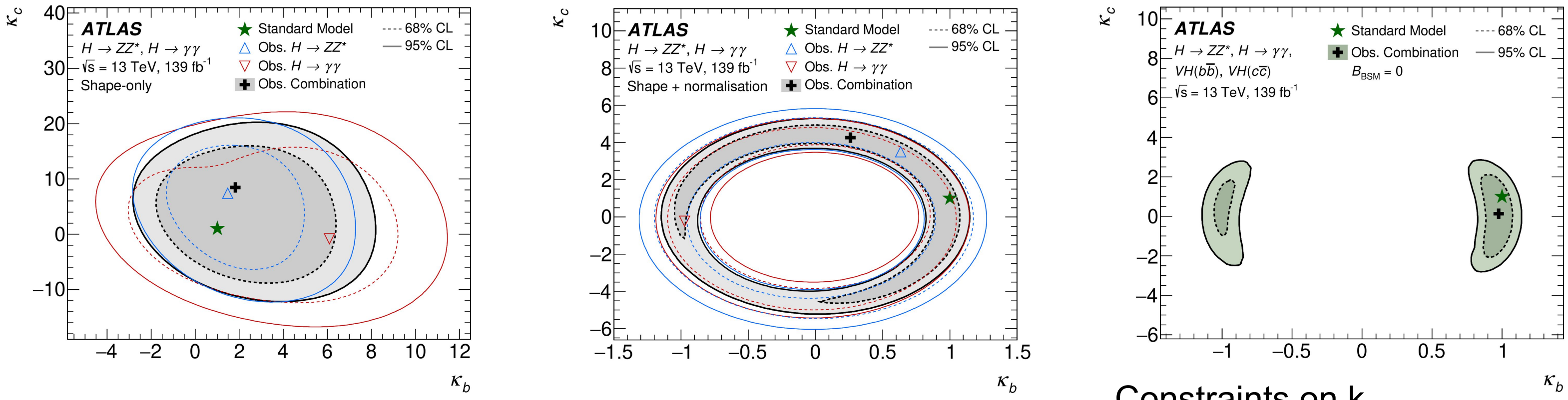


A combined fit with VHbb and VHcc measurements allows tighter constraints on $k_c$, which are the most stringent in this scenario

Constraints on $k_c$

| Scenario | Observed 68% confidence interval | Observed 95% confidence interval |
|---|---|---|
| $B_{\mathrm{BSM}} = 0$ | [−1.61, 1.70] | [−2.47, 2.53] |
| No assumption on $B_{\mathrm{BSM}}$ | [−2.63, 3.01] | [−4.46, 4.81] |

# H→ZZ (4l) and H→ γγ at 13.6 TeV - here we go again

New early Run3 combination - first measurement at the new centre-of-mass energy

Eur. Phys. J. C 84 (2024) 78

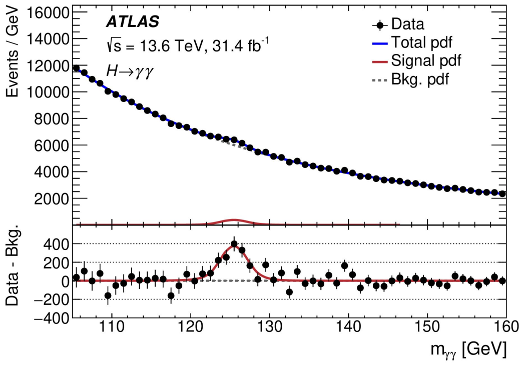


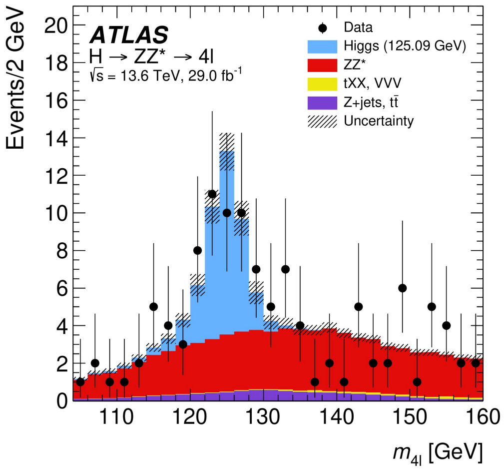


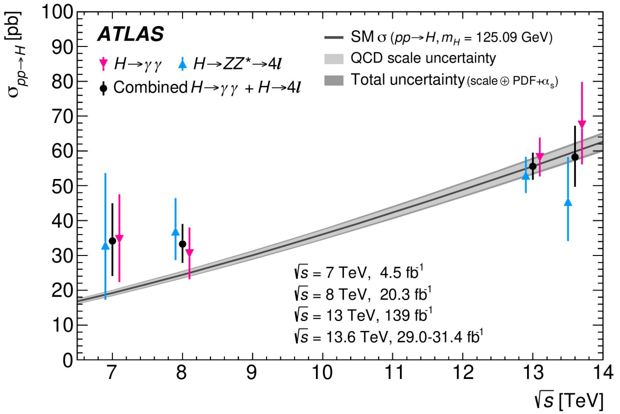


Individual and combined results comparable with the SM predictions

$\sigma(pp \rightarrow H) = 58.2 \pm 8.7$ fb vs $\sigma(pp \rightarrow H)_{SM} = 59.9 \pm 2.6$ fb

# (ggF and VBF) H→WW - differential cross section

Higher branching ratio but worse resolution

ggF

Eur. Phys. J. C 83 (2023) 774

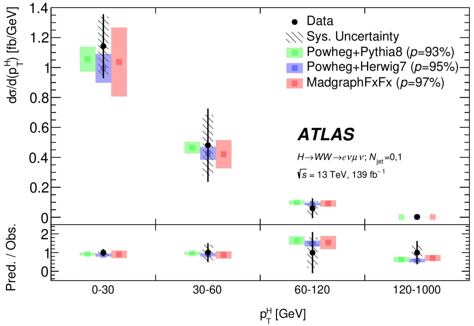


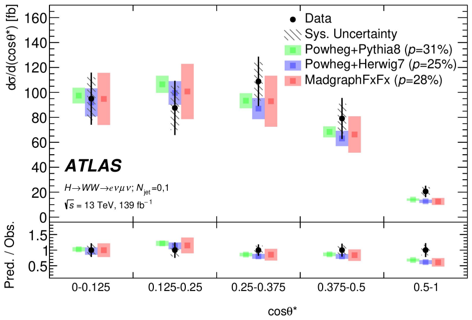


Measured single- and double-differential cross sections. $\cos\theta^*$ sensitive to the spin structure of the dilepton system

VBF

Phys. Rev. D 108 (2023) 072003

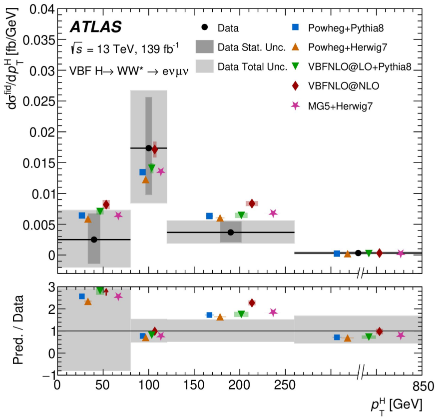


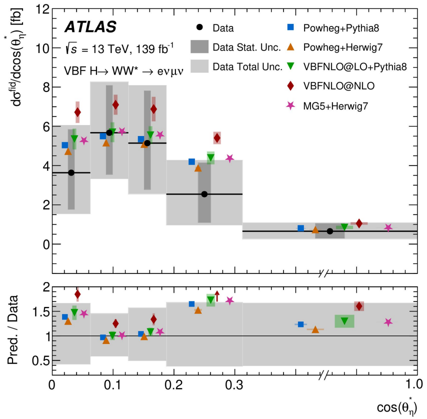


Good agreement with the SM predictions within uncertainties

# ggF H→WW - double differential cross section

[Eur. Phys. J. C 83 (2023) 774]

Six double differential cross sections as a function of kinematic variables (sensitive to the production kinematics) and jet multiplicity (up to one jet, sensitive to the decay kinematics)

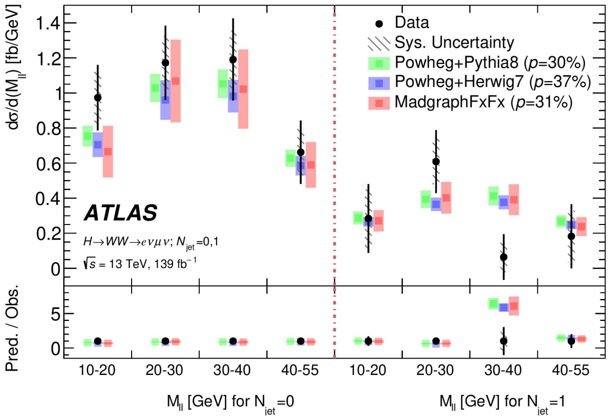


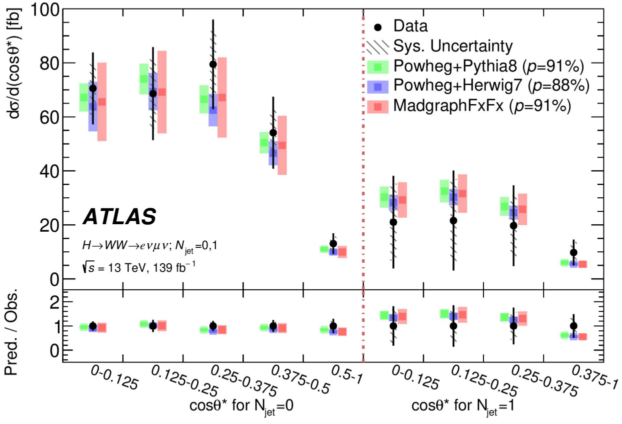


Compatibility with the data expressed with p-values. Good agreement with the SM expectations

# VBF H→WW - fiducial cross section

[Phys. Rev. D 108 (2023) 072003]

Cross section overestimated by 15-28% by the predictions at NLO or at LO with parton shower, although compatible at the level of ~1σ. Fixed-order calculation of VBFNLO@LO overestimates other predictions by 24%

| Simulation Name | Generator | ME Accuracy | PDF | Shower & Hadronization | UE & PS Parameter Set |
|---|---|---|---|---|---|
| Powheg+Pythia 8 | POWHEG-BOX v2 | NLO QCD & EW + approx. NNLO QCD | NNPDF3.0NLO | Pythia 8.230 +EvtGen v1.6.0 | AZNLO |
| Powheg+Herwig 7 | POWHEG-BOX v2 | NLO QCD & EW + approx. NNLO QCD | NNPDF3.0NLO | Herwig 7.1.3 +EvtGen v1.6.0 | H7UE |
| MG5+Herwig 7 | MadGraph5_aMC@NLO | NLO QCD, LO EW | NNPDF30NLO | Herwig 7.1.6 EvtGen v1.7.0 | H7UE |
| VBFNLO@LO | VBFNLO 2.7.1 | LO QCD & EW | NNPDF3.0NLO CT14, MMHT14 | - | - |
| VBFNLO@NLO | VBFNLO 2.7.1 | NLO QCD & EW | NNPDF3.0NLO CT14, MMHT14 | - | - |
| VBFNLO@LO+Pythia 8 | VBFNLO 2.7.1 | LO QCD & EW | NNPDF3.0NLO CT14, MMHT14 | Pythia 8.244 +EvtGen v1.7.0 | A14 |

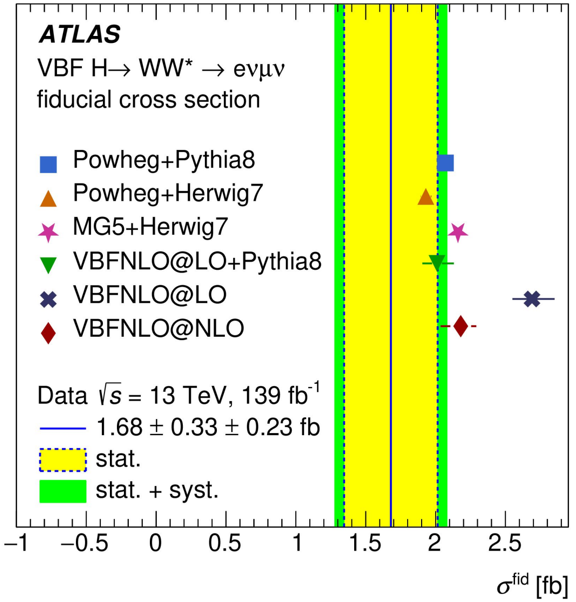

# (ggF+VBF) H→WW - STXS measurement

Phys. Rev. D 108 (2023) 032005

Measured cross section in ggF (VBF) production mode probes couplings to heavy quarks (W and Z). Performed in different jet multiplicity regions

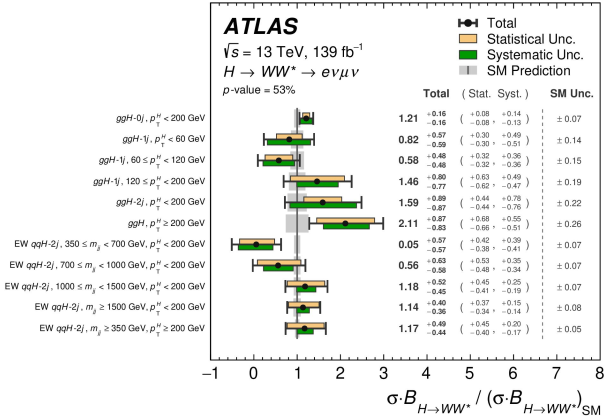


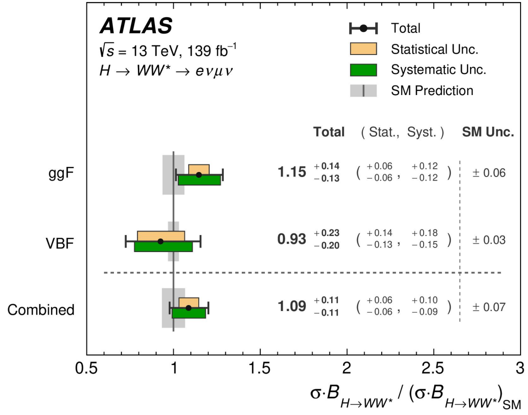


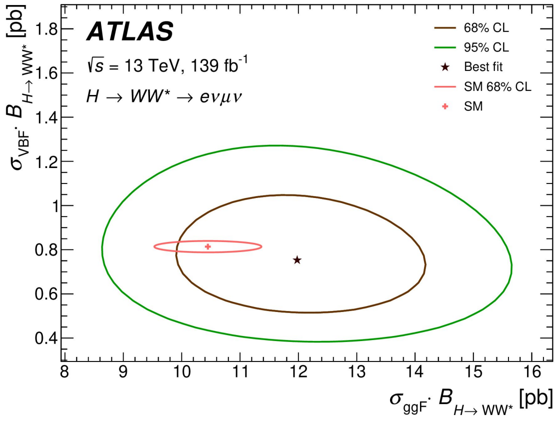


Both ggF and VBF cross sections multiplied by the branching ratio are in agreement with the SM

# EFT interpretation

arXiv:2402.05742

Can reflect the effect from a wide class of BSM theories and provide a common language to describe the BSM effect in all the Higgs analyses

$$\mathcal{L}_{\text{SMEFT}} = \mathcal{L}_{\text{SM}} + \sum_i^{N_{d=6}} \frac{c_i}{\Lambda^2} O_i^{(6)} + \sum_j^{N_{d=8}} \frac{b_j}{\Lambda^4} O_j^{(8)} + \ldots, \qquad (\sigma\times\mathcal{B})^{i,k',H\to X}_{\text{SMEFT}} = \sigma^{i,k'}_{\text{SMEFT}} \times \mathcal{B}^{H\to X}_{\text{SMEFT}} = \left(\sigma^{i,k'}_{\text{SM}} + \sigma^{i,k'}_{\text{int}} + \sigma^{i,k'}_{\text{BSM}}\right) \times \left(\frac{\Gamma^{H\to X}_{\text{SM}} + \Gamma^{H\to X}_{\text{int}} + \Gamma^{H\to X}_{\text{BSM}}}{\Gamma^{H}_{\text{SM}} + \Gamma^{H}_{\text{int}} + \Gamma^{H}_{\text{BSM}}}\right)$$

Linear term: interference between dim-6 operators and SM; Quadratic term: Pure BSM, product of two dim-6 amplitudes

| Decay channel | Analysis Production mode | $\mathcal{L}$ [fb$^{-1}$] | Reference | Binning | SMEFT | 2HDM and (h)MSSM |
|---|---|---|---|---|---|---|
| $H\to\gamma\gamma$ | (ggF, VBF, $WH$, $ZH$, $t\bar{t}H$, $tH$) | 139 | [38] | STXS-1.2 | ✓ | ✓ |
| | | | [19] | differential | ✓(subset) | |
| $H\to ZZ^*$ | ($ZZ^*\to 4\ell$: ggF, VBF, $WH+ZH$, $t\bar{t}H+tH$) | 139 | [22] | STXS-1.2 | ✓ | ✓ |
| | | | [18] | differential | ✓(subset) | |
| | ($ZZ^*\to \ell\ell\nu\bar{\nu}/\ell\ell q\bar{q}$: $t\bar{t}H$ multileptons) | 36.1 | [27] | STXS-0$^*$ | | ✓ |
| $H\to\tau\tau$ | (ggF, VBF, $WH+ZH$, $t\bar{t}H+tH$) | 139 | [39] | STXS-1.2 | ✓ | ✓ |
| | ($t\bar{t}H$ multileptons) | 36.1 | [27] | STXS-0$^*$ | | ✓ |
| $H\to WW^*$ | (ggF, VBF) | 139 | [40] | STXS-1.2 | ✓ | ✓ |
| | ($WH$, $ZH$) | 36.1 | [41] | STXS-0$^*$ | | ✓ |
| | ($t\bar{t}H$ multileptons) | 36.1 | [27] | STXS-0$^*$ | | ✓ |
| $H\to bb$ | ($WH$, $ZH$) | 139 | [42,25] | STXS-1.2 | ✓ | ✓ |
| | (VBF) | 126 | [43] | STXS-1.2 | ✓ | ✓ |
| | ($t\bar{t}H+tH$) | 139 | [44] | STXS-1.2 | ✓ | ✓ |
| | (boosted Higgs bosons: inclusive production) | 139 | [45] | STXS-1.2 | ✓ | ✓ |
| $H\to Z\gamma$ | (inclusive production) | 139 | [46] | STXS-0$^*$ | ✓ | ✓ |
| $H\to\mu\mu$ | (ggF $+t\bar{t}H+tH$, VBF $+WH+ZH$) | 139 | [47] | STXS-0$^*$ | ✓ | ✓ |

# EFT interpretation of combined STXS measurements

arXiv:2402.05742

Fit basis expressed in terms of single Warsaw basis coefficients $c_j$ and in terms of linear combinations ($e$) of coefficients to achieve both fit stability and fit-parameter interpretability

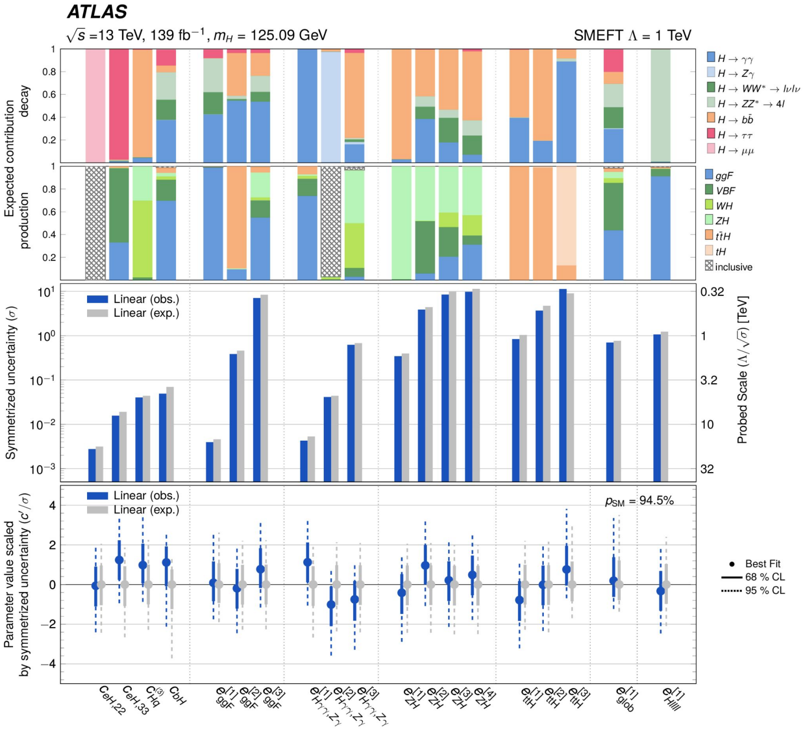


Good agreement with SM, obs. uncertainties are generally smaller than the exp. ones

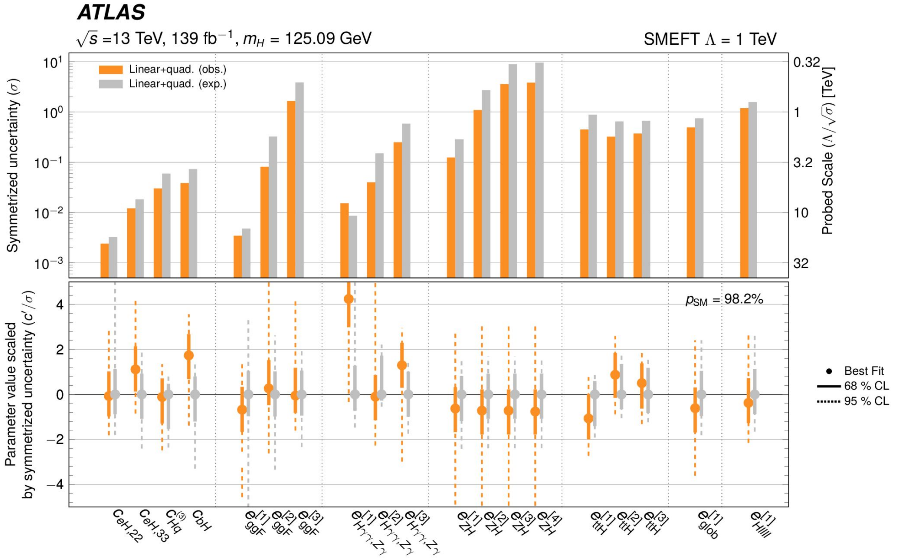

# EFT based on differential measurements

arXiv:2402.05742

Differential distributions (fiducial cross sections and STXS) provide more information on the final state kinematics, giving additional constraint power to Wilson coefficients

Constraints on the anomalous Higgs coupling to gluons and top quarks set from the observed $p_T^H$ spectra in the $H \rightarrow ZZ \rightarrow 4l$ and $H \rightarrow \gamma\gamma$ channels

Differential cross-section measurements show less constraining power than the STXS measurements, as they probe the distribution of a single observable inclusively in production mode (unlike STXS measurements)

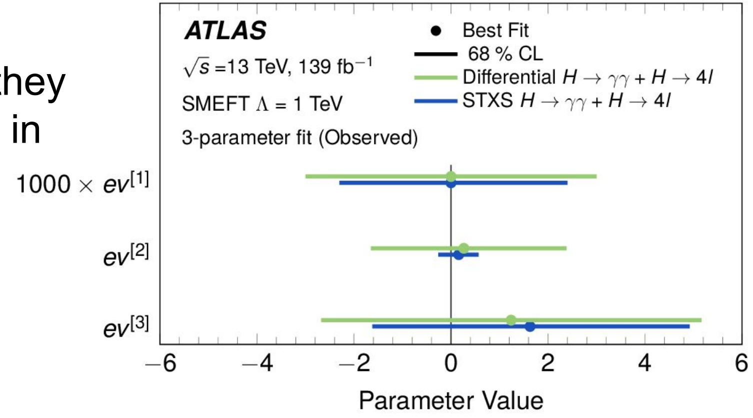


$ev^{[1,2,3]}$ related to the Wilson coefficients ($c_{HG}$, $c_{tG}$ and $c_{tH}$) through a rotation in the parameter space so to probe them simultaneously

# VBF H→WW - EFT interpretation

[Phys. Rev. D 108 (2023) 072003]

Wilson coefficients obtained from different differential distributions. Fitted one-at-a-time
Stringent constraints set to many EFT parameters, especially when the quadratic term is added (sensitive to neglected contributions of higher-dimensional operators in the EFT expansion)

**CP-even operators**

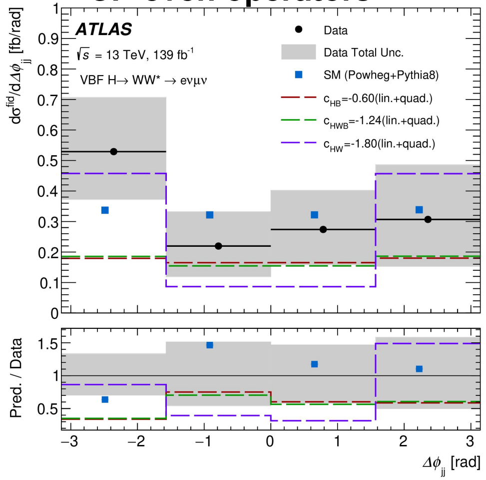


**CP-odd operators**

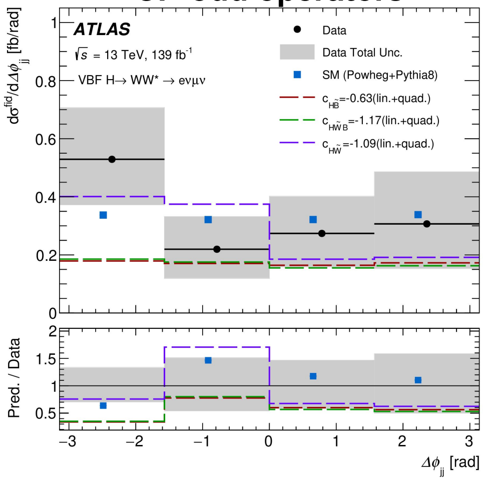


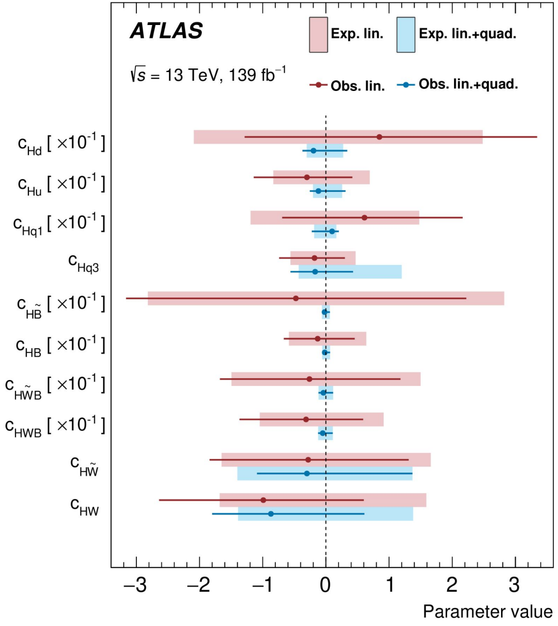

# Summary

Lots of exciting differential measurements and EFT interpretations

Measurements of the production mode cross sections, STXS, fiducial differential cross sections reparametrised in terms of SMEFT and provided new constraints on the Wilson coefficients

First measurement at 13.6 TeV, more will be published in the near future

Looking forward to seeing the new measurements and producing updated EFT interpretation

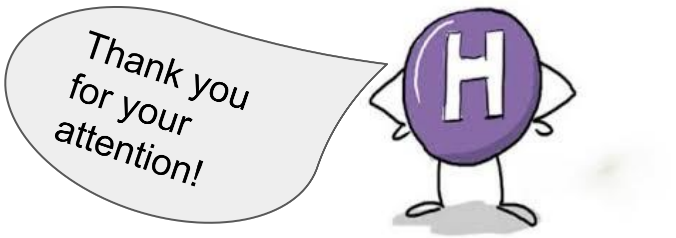

# Backup

# EFT interpretation of STXS measurements

## Linear model

$$
\begin{aligned}
(\sigma\times\mathcal{B})^{i,k',H\to X}_{\text{SMEFT}} &= (\sigma\times\mathcal{B})^{i,k',H\to X}_{\text{SM},((\text{N})\text{N})\text{NLO}} \times \left(1 + \frac{\sigma^{i,k'}_{\text{int},(\text{N})\text{LO}}}{\sigma^{i,k'}_{\text{SM},(\text{N})\text{LO}}}\right) \times \left(\frac{1 + \frac{\Gamma^{H\to X}_{\text{int}}}{\Gamma^{H\to X}_{\text{SM}}}}{1 + \frac{\Gamma^{H}_{\text{int}}}{\Gamma^{H}_{\text{SM}}}}\right) \\
&= (\sigma\times\mathcal{B})^{i,k',H\to X}_{\text{SM},((\text{N})\text{N})\text{NLO}} \times \left(1 + \sum_j A_j^{\sigma_{i,k'}} c_j\right) \times \left(\frac{1 + \sum_j A_j^{\Gamma^{H\to X}} c_j}{1 + \sum_j A_j^{\Gamma^H} c_j}\right), \\
&= (\sigma\times\mathcal{B})^{i,k',H\to X}_{\text{SM},((\text{N})\text{N})\text{NLO}} \times \left(\frac{1 + \sum_j \left(A_j^{\sigma_{i,k'}} + A_j^{\Gamma^{H\to X}}\right) c_j + O\left(\Lambda^{-4}\right)}{1 + \sum_j A_j^{\Gamma^H} c_j + O\left(\Lambda^{-4}\right)}\right),
\end{aligned}
$$

$$
\frac{\sigma^{i,k'}_{\text{int}}}{\sigma^{i,k'}_{\text{SM}}} = \sum_j A_j^{\sigma_{i,k'}} c_j \qquad \frac{\sigma^{i,k'}_{\text{BSM}}}{\sigma^{i,k'}_{\text{SM}}} = \sum_{j,l\geq j} B_{jl}^{\sigma_{i,k'}} c_j c_l
$$

$$
\frac{\Gamma^{H\to X}_{\text{int}}}{\Gamma^{H\to X}_{\text{SM}}} = \sum_j A_j^{\Gamma^{H\to X}} c_j \qquad \frac{\Gamma^{H\to X}_{\text{BSM}}}{\Gamma^{H\to X}_{\text{SM}}} = \sum_{j,l\geq j} B_{jl}^{\Gamma^{H\to X}} c_j c_l
$$

$$
\frac{\Gamma^{H}_{\text{int}}}{\Gamma^{H}_{\text{SM}}} = \sum_j A_j^{\Gamma^{H}} c_j \qquad \frac{\Gamma^{H}_{\text{BSM}}}{\Gamma^{H}_{\text{SM}}} = \sum_{j,l\geq j} B_{jl}^{\Gamma^{H}} c_j c_l,
$$

$$
A_j^{\Gamma^H} = \frac{\sum_X \Gamma^{H\to X}_{\text{SM}} A_j^{\Gamma^{H\to X}}}{\sum_X \Gamma^{H\to X}_{\text{SM}}} \qquad B_{jl}^{\Gamma^H} = \frac{\sum_X \Gamma^{H\to X}_{\text{SM}} B_{jl}^{\Gamma^{H\to X}}}{\sum_X \Gamma^{H\to X}_{\text{SM}}}.
$$

## Quadratic model

$$
\begin{aligned}
(\sigma\times\mathcal{B})^{i,k',H\to X}_{\text{SMEFT}} &= (\sigma\times\mathcal{B})^{i,k',H\to X}_{\text{SM},((\text{N})\text{N})\text{NLO}} \left(1 + \sum_j A_j^{\sigma_{i,k'}} c_j + \sum_{j,l\geq j} B_{jl}^{\sigma_{i,k'}} c_j c_l\right)\left(\frac{1 + \sum_j A_j^{\Gamma^{H\to X}} c_j + \sum_{j,l\geq j} B_{jl}^{\Gamma^{H\to X}} c_j c_l}{1 + \sum_j A_j^{\Gamma^{H}} c_j + \sum_{j,l\geq j} B_{jl}^{\Gamma^{H}} c_j c_l}\right), \\
&= (\sigma\times\mathcal{B})^{i,k',H\to X}_{\text{SM},((\text{N})\text{N})\text{NLO}} \cdot \\
&\left(\frac{1 + \sum_j \left(A_j^{\sigma_{i,k'}} + A_j^{\Gamma^{H\to X}}\right) c_j + \sum_{j,l}\left(A_j^{\sigma_{i,k'}} A_l^{\Gamma^{H\to X}}\right) c_j c_l + \sum_{j,l\geq j}\left(B_{jl}^{\sigma_{i,k'}} + B_{jl}^{\Gamma^{H\to X}}\right) c_j c_l + O\left(\Lambda^{-6}\right)}{1 + \sum_j \left(A_j^{\Gamma^H}\right) c_j + \sum_{j,l\geq j}\left(B_{jl}^{\Gamma^H}\right) c_j c_l + O\left(\Lambda^{-6}\right)}\right) \quad (13)
\end{aligned}
$$

# EFT interpretation of STXS measurements

Eigenvectors obtained from the expected measurements accounting for the observed values of nuisance parameters, ranked by eigenvalue and truncated to eigenvalues $\boldsymbol{\lambda}_i \geq 0.01$

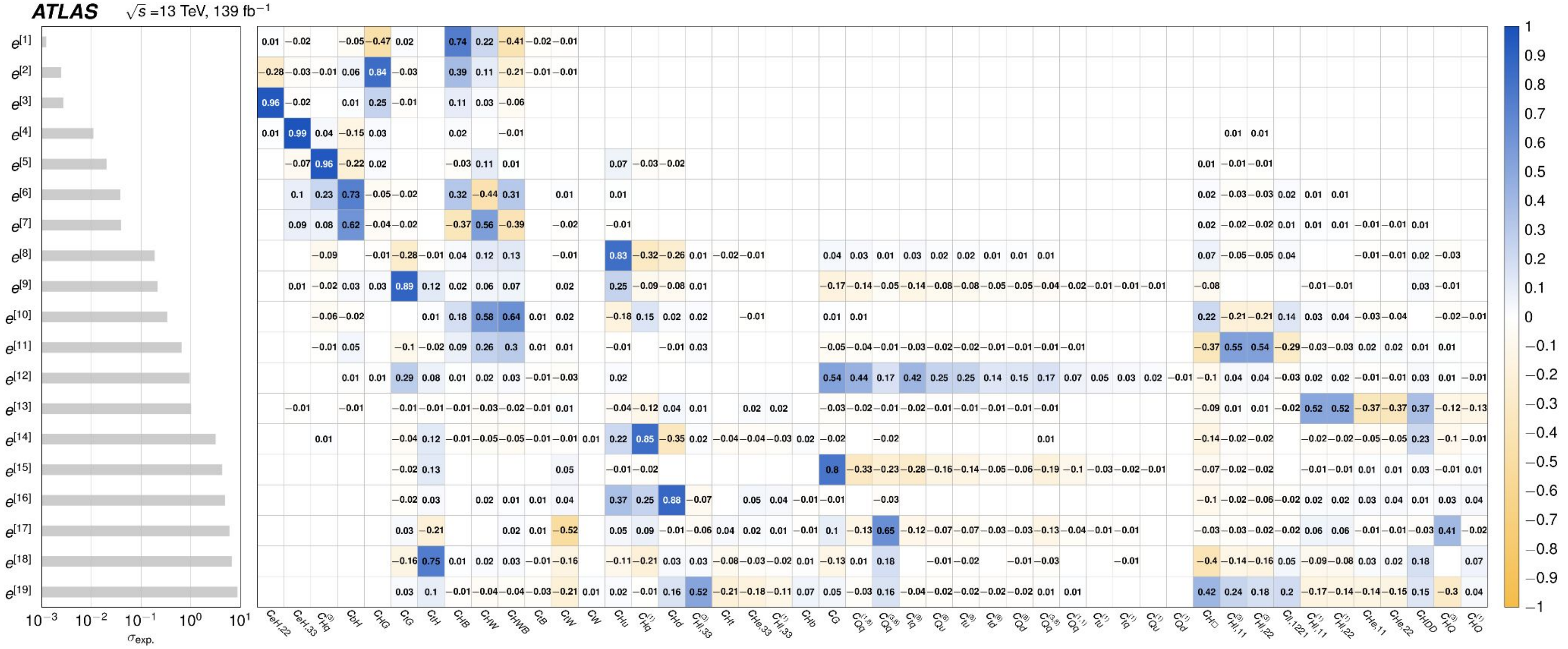

# EFT interpretation of STXS measurements

Definition of the fit basis coefficients $\boldsymbol{c}'$ in terms of the Warsaw basis coefficients $\boldsymbol{c}$

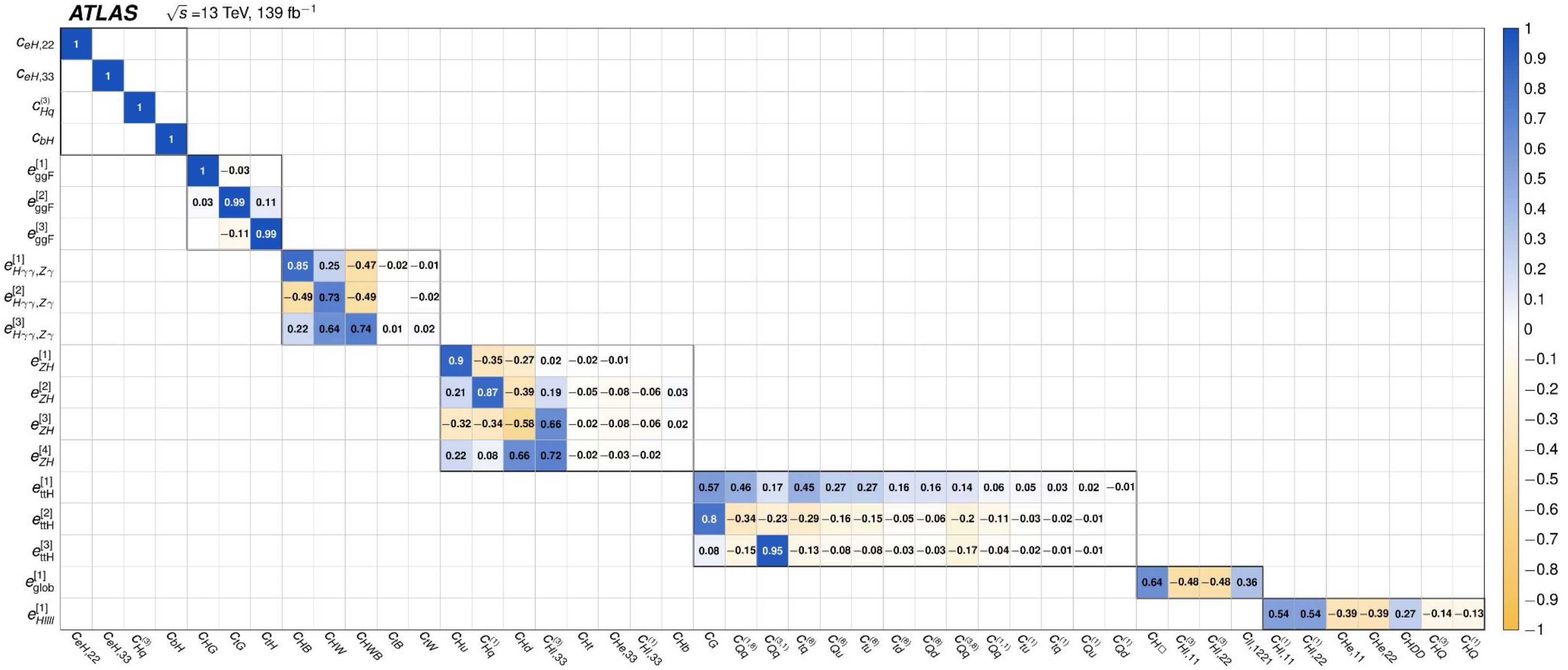

# EFT interpretation of STXS measurements

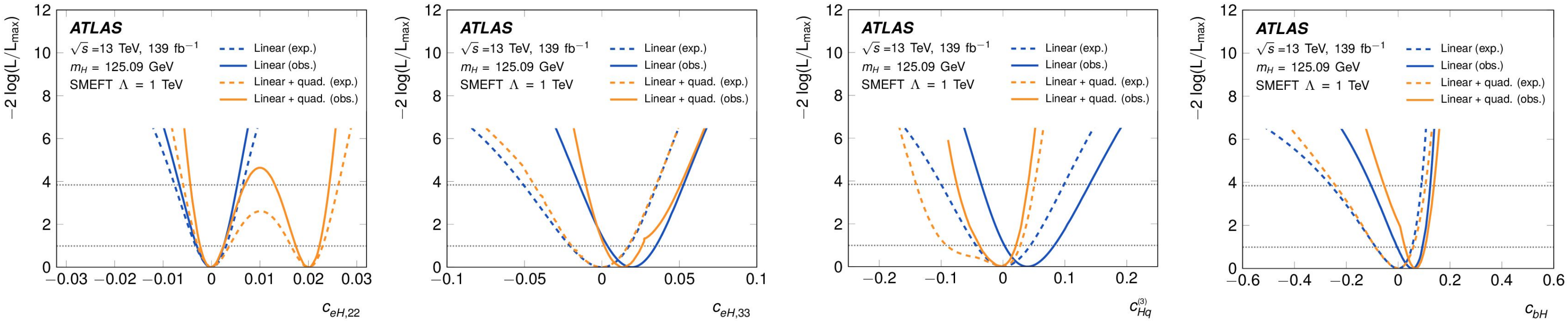

# EFT interpretation of STXS measurements

Constraints from the quadratic terms are significantly stronger. These arise from the relatively weak impact of the BSM–SM interference term on the cross-section compared to the quadratic BSM terms in specific production or decay modes

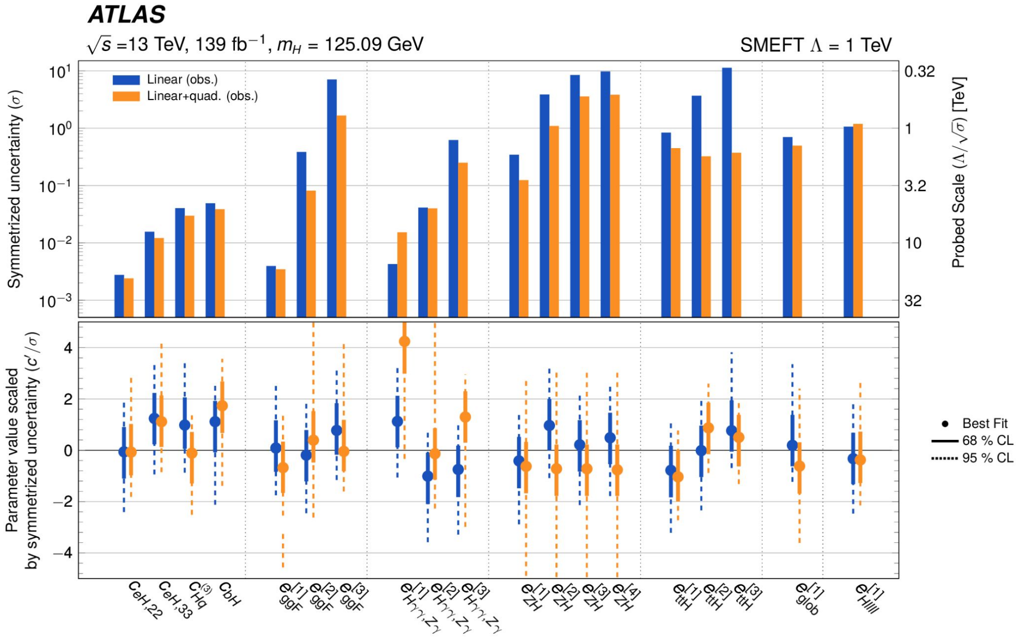

# H->ZZ (4l) and H->yy - Fiducial cross section

| | |
|---|---|
| **Lepton and jet definitions** | |
| Leptons | Dressed leptons not originating from hadron or $\tau$ decays |
| | $p_{\mathrm{T}} > 5$ GeV, $\lvert\eta\rvert < 2.7$ |
| Jets | $p_{\mathrm{T}} > 30$ GeV, $\lvert y\rvert < 4.4$ |
| **Lepton selection and pairing** | |
| Lepton kinematics | $p_{\mathrm{T}}$ threshold for three leading leptons: $> 20, 15, 10$ GeV |
| Leading pair ($m_{12}$) | SFOC lepton pair with smallest $\lvert m_Z - m_{\ell\ell}\rvert$ |
| Subleading pair ($m_{34}$) | Remaining SFOC lepton pair with smallest $\lvert m_Z - m_{\ell\ell}\rvert$ as nominal |
| **Event selection** | |
| Mass requirements | 50 GeV$< m_{12} <$ 106 GeV and 12 GeV$< m_{34} <$ 115 GeV |
| Lepton separation | $\Delta R(\ell_i, \ell_j) > 0.1$ |
| Lepton/Jet separation | $\Delta R(\ell_i, \mathrm{jet}) > 0.1$ |
| $J/\psi$ veto | $m(\ell_i, \ell_j) > 5$ GeV for all SFOC lepton pairs |
| Mass window | 105 GeV$< m_{4\ell} <$ 160 GeV |
| If extra lepton with $p_{\mathrm{T}} > 12$ GeV | Quadruplet with largest ggF matrix element value |

| | |
|---|---|
| **Photon and jet definitions** | |
| Photons | Photons not originating from hadron decays |
| | $p_{\mathrm{T}} > 15$ GeV, $\lvert\eta\rvert < 1.37$ or $1.52 < \lvert\eta\rvert < 2.37$ |
| | $E_{\mathrm{T}}^{\mathrm{iso}}(\Delta R < 0.2, p_{\mathrm{T}} > 1$ GeV, charged$) < 0.05\, E_{\mathrm{T}}$ |
| Jets | $p_{\mathrm{T}} > 30$ GeV, $\lvert y\rvert < 4.4$ |
| **Event selection** | |
| Photon kinematics | $p_{\mathrm{T}}$ threshold for two leading photons: $p_{\mathrm{T}}^{\gamma_1} > 0.35 m_{\gamma\gamma}$, $p_{\mathrm{T}}^{\gamma_2} > 0.25 m_{\gamma\gamma}$ |
| Mass window | 105 GeV $< m_{\gamma\gamma} <$ 160 GeV |

# H->ZZ (4l) and H->yy - Acceptance factors

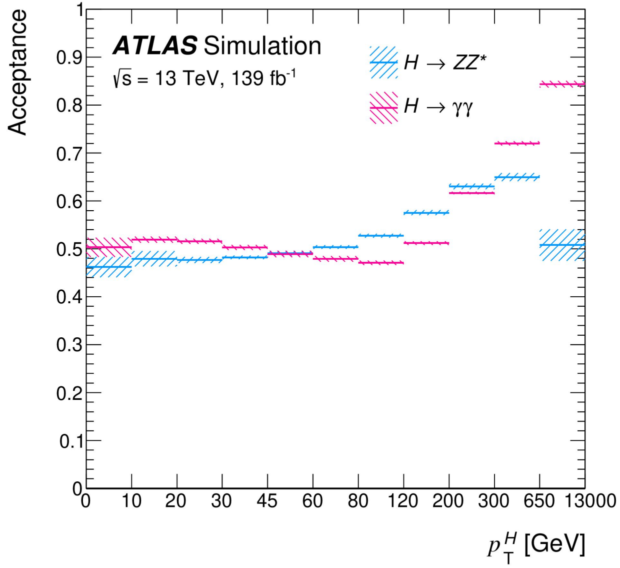


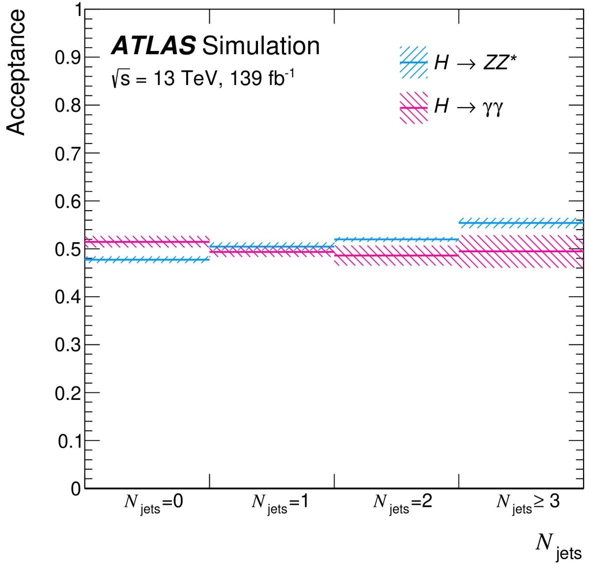

# EFT based on differential measurements

arXiv:2402.05742

$$
\begin{aligned}
ev^{[1]} &= \ \ 0.999c_{HG} - 0.035c_{tG} - 0.003c_{tH}, \\
ev^{[2]} &= \ \ 0.035c_{HG} + 0.978c_{tG} + 0.205c_{tH}, \\
ev^{[3]} &= -0.005c_{HG} - 0.205c_{tG} + 0.979c_{tH}.
\end{aligned}
$$